Steel and Composite Structures, *Vol. 29, No. 3 (2018) 333-348*
DOI: https://doi.org/10.12989/scs.2018.29.3.333

Contact buckling behaviour of corrugated plates subjected to linearly varying in-plane loads

Jianghui Dong [a], Xing Ma [*], Yan Zhuge [b] and Julie E. Mills [c]

School of Natural and Built Environments, University of South Australia, Adelaide, SA 5095, Australia

(*Received February 26, 2018, Revised July 3, 2018, Accepted July 7, 2018*)

Abstract. An analytical method is developed for analysing the contact buckling response of infinitely long, thin corrugated plates and flat plates restrained by a Winkler tensionless foundation and subjected to linearly varying in-plane loadings, where the corrugated plates are modelled as orthotropic plates and the flat plates are modelled as isotropic plates. The critical step in the presented method is the explicit expression for the lateral buckling mode function, which is derived through using the energy method. Simply supported and clamped edges conditions on the unloaded edges are considered in this study. The acquired lateral deflection function is applied to the governing buckling equations to eliminate the lateral variable. Considering the boundary conditions and continuity conditions at the border line between the contact and non-contact zones, the buckling coefficients and the corresponding buckling modes are found. The analytical solution to the buckling coefficients is also expressed through a fitted approximate formula in terms of foundation stiffness, which is verified through previous studies and finite element (FE) method.

Keywords: linearly varying in-plane loading; contact buckling; buckling coefficient; Winkler tensionless foundation; finite element analysis

1. Introduction

Corrugated plates are structural components that have been widely used in engineering fields including civil engineering, marine industries, aircraft manufacturing and mechanical industries. As the load carrying members, the corrugated plates subjected to various loads, such as compression, in-plane shear, linearly varying in-plane loads and combinations of these. Local buckling is one of the major governing design criteria in engineering practise for corrugated plates.

A number of researchers have studied local buckling behaviour of flat plates under linearly varying in-plane loads using various methods. In 1937, Nölke (1937) used the energy method to develop the first exact solution to critical buckling coefficients of square plates subjected to linearly varying in-plane loadings (two cases were considered, i.e. loading factor α = 1 and 2). In 1961, the exact buckling coefficients for square plates with simply supported edges for various loading conditions (i.e., α = 0, 2/3, 4/5, 1, 4/3 and 2) were determined by Timoshenko and Gere (1961). Based on the study of Nölke (1937), Bulson (1970) summarized the critical buckling coefficients of square plates with both clamped and simply supported edges under various loading conditions including α = 0, α = 0.5, α = 1, α = 1.5 and α = 2. In recent studies, (Leissa and Kang 2002, Kang and Leissa 2005), various boundary conditions were considered, such as plates with two edges simply supported and two edges clamped and plates simply supported on all edges. The exact buckling solution to a finite long rectangular plate under linearly varying in-plane loads (α = 0, α = 1 and α = 2) was obtained through a differential quadrature method (Wang *et al*. 2006). Schuette and McCulloch (1947) studied the buckling problem of long plates under pure bending, and with elastically restrained edges.

In composite plates, the buckling behaviour of the skin is different because of the support from the core material, which is usually modelled as tensionless foundations if debonding occurs between skin elements and core materials. This kind of buckling phenomenon is also known as contact buckling. Seide (1958) analysed the isotropic plate buckling problem supported on tensionless elastic foundations. Smith et al. carried out investigations on the compressive buckling and shearing buckling of isotropic flat plates resting on tensionless foundations (Smith *et al*. 1999a, b, c, d, Bradford *et al*. 2000). Shahwan and Waas (1994) developed a contact buckling model for orthotropic plates under compression. Wright (1995) used the energy method to address the local buckling problem of steel on rigid foundations and subjected to bending, axial, shearing forces and combinations of these. Smith *et al*. (2000) reported on the unilateral local buckling behaviour of steel plates on rigid foundations under bending using the Ritz energy method. Recent study (Li *et al*. 2016) revealed the boundary condition at the loaded edges (end conditions) significantly affected the contact buckling performance. The

*Corresponding author, Ph.D., Senior Lecturer,
E-mail: Xing.Ma@unisa.edu.au
[a] Ph.D., E-mail: jianghui.dong@mymail.unisa.edu.au
[b] Professor, E-mail: yan.zhuge@unisa.edu.au
[c] Professor, E-mail: julie.mills@unisa.edu.au

ISSN: 1229-9367 (Print), 1598-6233 (Online)

buckling of profiled sheets was analysed on rigid foundations (Ma *et al*. 2008b, Dong et al. 2018a) and elastic tensionless foundations (Dong *et al*. 2016b, a, 2018b). The compressive and shear buckling problem of laminated composite plate on one-sided foundations was studied by Dong *et al*. (2017, 2018c). In addition, Altunsaray and Bayer (2014) using Galerkin and finite difference method to analyse the buckling problem of symmetrically laminated plate. The higher order shear deformation plate theory (Baseri *et al*. 2016) and nth-order shear deformation theory (Becheri *et al*. 2016) were used to implement the buckling of laminated plates. As practical applications, Liang *et al*. (2003, 2004) studied the local buckling and post-local buckling behaviour of steel skins in composite panels under biaxial compression and its combination with shear loads.

However, the above studies on contact buckling analysis mostly focused on the loads of compression, shear and their combinations. To the best knowledge of the authors, the contact buckling problem for plates supported by elastic tensionless foundations under linearly varying in-plane loads including pure bending has not been studied in the existing literature. Unlike the pure compressive loading, the linearly varying in-plane loads are complicated. For the pure compressive loading, the lateral buckling mode function can be assumed as one term trigonometric function, while more than one term trigonometric or hyperbolic function has to be used to express lateral buckling mode function when the plate under linearly varying in-plane loads.

This paper addresses the contact buckling behaviour of thin corrugated plate under linearly varying in-plane loads. The flat plate can be regarded as a special case of the corrugated plates. Both analytical solutions and FEM solutions are presented.

2. Governing formulations

2.1 Buckling model

The buckling mode of an infinitely long corrugated sheet resting on a tensionless foundation and loaded by linearly varying in-plane loads is shown in Fig. 1, where two unknown areas (i.e., contact and non-contact areas) can be expected.

The governing equation for this problem may be expressed as (Timoshenko and Woinowsky-Krieger 1959, Timoshenko and Gere 1961)

$$\begin{aligned} &D_x w_{i,x_i x_i x_i x_i} + 2H w_{i,x_i x_i yy} + D_y w_{i,yyyy} \\ &+N_x w_{i,x_i x_i} + 2N_{xy} w_{i,x_i y} + N_y w_{i,yy} = q_i \quad |x_i| \le a_i/2 \end{aligned} \tag{1}$$

where w is the transverse displacement; D_x, D_y, and H are the flexural stiffness and defined in Eq. (2); N_x, N_y and N_{xy} are the in-plane loads and N_x is defined in Eq. (3); q_i is the force between the plate and foundation and defined in Eq. (4).

The stiffness of the corrugated plate can be calculated using the following equations (Xia *et al*. 2012, Ye *et al*. 2014)

$$D_x = \frac{1}{c}\left(I_1 \frac{E^s t^3}{12(1-v^{s2})} + I_x \frac{E^s}{1-v^{s2}}\right) \tag{2a}$$

$$D_y = \frac{c}{s}\frac{E^s t^3}{12(1-v^{s2})} \tag{2b}$$

$$H = D_{12} + 2D_{xy} = \frac{v^s E^s t^3}{12(1-v^{s2})} + \frac{E^s t^3 s}{12(1+v^s)c} \tag{2c}$$

$$I_1 = \int_0^s \left(\frac{dy}{ds}\right)^2 ds \tag{2d}$$

where E^s, t, v^s are the elastic modulus, thickness and Poisson's ratio of the skin sheet, respectively. I_x, c and s are the inertia moment of the cross-section, width and arc length along the corrugated cross section of a repeating corrugation, respectively (Fig. 1).

For linearly varying in-plane load, $N_y = N_{xy} = 0$, N_x and the buckling coefficient can be expressed as

$$N_x = N_0\left(1 - \alpha\frac{y}{b}\right) \tag{3a}$$

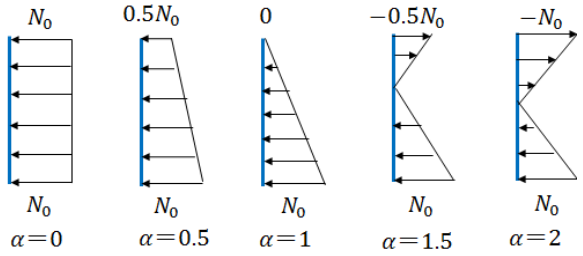

Fig. 2 Load patterns (N_x) for right loading edge

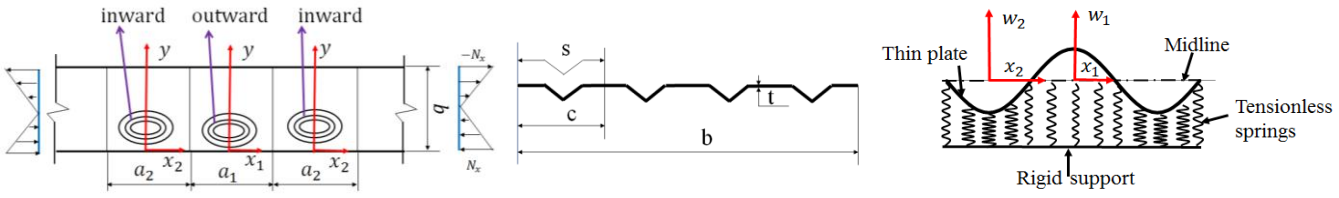

(a) (b) (c)

Fig. 1 Schematic diagram of the plate under linearly varying in-plane loading: (a) bucking mode of an infinite plate; (b) cross section of corrugated plate; and (c) tensionless foundation represented by tensionless springs

$$K = \frac{b^2 N_0}{\pi^2 D_y} = \frac{b^2 t \sigma_0}{\pi^2 D_y} \tag{3b}$$

where N_0 is the maximum value of the distributed loads and α is the loading parameter, equal to 1 minus the stress gradient coefficient (the ratio of edge stresses). Various cases may be obtained through changing the value of α (Fig. 2). By taking α = 0, a case with uniaxial uniformly distributed compression may be gained. When α = 1, the load is a triangular distribution load, the value is N_0 at y = 0 and 0 at y = b. For α = 2, a pure bending case may be gained. If 0 < α ≤ 1, the loading is non-uniform compression. If 1 < α < 2, one part of the plate is subjected to non-uniform compression and another part is subjected to non-uniform tension.

Considering $w_i(x_i, y) = f_i(x_i)g(y)$ and using a Winkler tensionless foundation to represent the elastic tensionless foundation, the following equation may be obtained

$$q_i(x_i, y) = -k_i f_i(x_i) g(y) \tag{4}$$

where i = 1 and 2, f_i and g are buckling mode functions in x and y directions, respectively, k_1 is zero for non-contact zones and k_2 is the Winkler foundation stiffness coefficient in contact zones. Thus, for contact zones, the contact pressure between plate and foundation is $k_2 f_2 g$, and for the non-contact zones, the contact force is zero.

Thus, Eq. (1) can be rewritten as

$$D_x f_i'''' g + 2H f_i'' g'' + D_y f_i g'''' + N_x f_i'' g = -k_i f_i g \tag{5}$$

where the superscript ‘ represents the differentiation with respect to x or y. ‘, “ and ““ are for the first derivative, the second derivative and the forth derivative, respectively.

After multiplying by $1/D_y$ on both sides, we have

$$\frac{D_x}{D_y} f_i'''' g + 2(1+r) f_i'' g'' + f_i g'''' + \frac{\pi^2 K}{b^2}\left(1 - \alpha\frac{y}{b}\right) f_i'' g = -\frac{k_i}{D_y} f_i g \tag{6}$$

where $r = \frac{H}{D_y} - 1$.

Multiplying both sides in Eq. (6) by $g(y)$ and taking the integral yields

$$\frac{D_x}{D_y} f_i'''' - \frac{1}{b^2}[B_1(1+r) - \pi^2 K B_2] f_i'' + \frac{1}{b^4}(B_3 + B_4) f_i = 0 \tag{7}$$

in which

$$B_1 = -\left\{ b^2 \int_0^b [2g'' g] dy \right\} \Big/ \int_0^b g^2 dy \tag{8a}$$

$$B_2 = \left\{ \int_0^b \left[\left(1 - \alpha\frac{y}{b}\right) g^2\right] dy \right\} \Big/ \int_0^b g^2 dy \tag{8b}$$

$$B_3 = b^4 \int_0^b g'''' g dy \Big/ \int_0^b g^2 dy \tag{8c}$$

$$B_4 = b^4 \int_0^b \frac{k_i}{D_y} g^2 dy \Big/ \int_0^b g^2 dy = \frac{b^4 k_i}{D_y} \tag{8d}$$

Assuming $f_1(x_1) = \tilde{f}_1(\xi_1)$, $\xi_1 = x_1/a_1$, $\gamma_1 = a_1/b$, $f_2(x_2) = \tilde{f}_2$, $\xi_2 = x_2/a_i$, $\gamma_2 = a_2/b$, $\tilde{k}_1 = 0$ and $\tilde{k}_2 = k_r > 0$, yields

$$\frac{D_x}{D_y} \tilde{f}_i'''' (\xi_i) - {\gamma_i}^2 [B_1(1+r) - \pi^2 K B_2] \tilde{f}_i'' (\xi_i) + B_3 {\gamma_i}^4 \left(1 + B_5 \tilde{k}_i\right) \tilde{f}_i(\xi_i) = 0 \tag{9}$$

in which

$$B_5 = \frac{B_4}{B_3 \times \tilde{k}_i} \tag{10}$$

2.2 Lateral buckling mode function

The elimination method was applied in this study which means that variable y will be eliminated and only x will be left in the equations. The selection of an appropriate lateral buckling mode function $g(y)$ is very important in the elimination method. Two boundary conditions on the two unloaded edges are considered in this study, i.e., clamped and simply supported.

2.2.1 Simply supported boundary condition

If the two unloaded edges are simply supported, the deflection function of an infinitely long plate without foundation can be given as Eq. (12). To determine the value of C_i, three cases have to be considered (Timoshenko and Gere 1961),

Case I α = 0, the load is pure compression, n can be selected as 1, C_1 may be assumed as 1, and the function and the second derivative of $g_1(y)$ should satisfy (Harris and Piersol 2002)

$$g_1(0) = g_1(b) = 0 \tag{11a}$$

$$g_1''(0) = g_1''(b) = 0 \tag{11b}$$

where the buckling mode of the plate can be expressed as

$$g = g_1 = \sin\left(\frac{\pi y}{b}\right) \tag{12}$$

Case II 0 < α < 2 (e.g., α = 1), the load is a combination of compression with bending, a satisfactory result can be obtained if n is selected as 2, and the function and the second derivative of $g_2(y)$ should satisfy (Harris and Piersol 2002)

$$g_2(0) = g_2\left(\frac{b}{2}\right) = g_2(b) = 0 \tag{13a}$$

$$g_2''(0) = g_2''(b) = 0 \tag{13b}$$

The buckling mode is

$$w(x,y)=\sin\left(\frac{\pi x}{\lambda}\right)\left[C_1\sin\left(\frac{\pi y}{b}\right)+C_2\sin\left(\frac{2\pi y}{b}\right)\right] \quad (14)$$

Considering the buckling mode in Eq. (14) and denoting $\phi = \lambda/b$, the elastic strain energy can be expressed as

$$U=\frac{D_y\pi^4}{8b^2\phi^3}\left[{C_1}^2\left(\frac{D_x}{D_y}+\phi^4+2\frac{\mathrm{H}}{D_y}\phi^2\right)+{C_2}^2\left(\frac{D_x}{D_y}+16\phi^4+8\frac{\mathrm{H}}{D_y}\phi^2\right)\right] \quad (15)$$

The work done by the external forces can be written as

$$V=-\frac{D_y\pi^4}{8b^2\phi^3}\left[K_x\left(1-\frac{\alpha}{2}\right)\left({C_1}^2+{C_2}^2\right)+32\alpha K_x\frac{C_1C_2}{9}\right] \quad (16)$$

$$\mathbf{BC}=0 \quad (17a)$$

where

$$\mathbf{B}=\begin{bmatrix}\left(\frac{D_x}{D_y}+\phi^4+2\frac{\mathrm{H}}{D_y}\phi^2\right)-K_x\phi^2\left(1-\frac{\alpha}{2}\right) & -\frac{16\alpha}{9\pi^2}K_x\phi^2\\ -\frac{16\alpha}{9\pi^2}K_x\phi^2 & \left(\frac{D_x}{D_y}+16\phi^4+8\frac{\mathrm{H}}{D_y}\phi^2\right)-K_x\phi^2\left(1-\frac{\alpha}{2}\right)\end{bmatrix} \quad (17b)$$

$$\mathbf{C}=\begin{bmatrix}C_1\\C_2\end{bmatrix} \quad (17c)$$

Since $\frac{H}{D_y}=r+1$, initially assume that the lateral buckling mode functions are the same for r= 0 and $r \neq 0$. The buckling coefficient K_{cr0} can be obtained for r= 0 and then the final buckling coefficient K_{cr} can be calculated for $r \neq 0$. Thus, first assume r= 0.

$$\mathbf{B}=\begin{bmatrix}\left(\frac{D_x}{D_y}+\phi^4+2\phi^2\right)-K_x\phi^2\left(1-\frac{\alpha}{2}\right) & -\frac{16\alpha}{9\pi^2}K_x\phi^2\\ -\frac{16\alpha}{9\pi^2}K_x\phi^2 & \left(\frac{D_x}{D_y}+16\phi^4+8\phi^2\right)-K_x\phi^2\left(1-\frac{\alpha}{2}\right)\end{bmatrix} \quad (17d)$$

The determinant of matrix B must be zero to get a non-trivial solution of Eq. (17). Considering $K=\frac{b^2N_0}{\pi^2D}$, the solution of K may be obtained. The value of K is a function of α and ϕ. In general, the value of α is given, thus, the minimum value of K_{cr0} may be obtained by solving $dK/d\phi$ = 0. Note that all critical buckling coefficients K_{cr0} are obtained based on r= 0. If D_x/D_y = 1 and α = 1, C_1 is assumed as 1, so C_2 can be calculated according to Eq. (17). C_i values can be obtained for D_x/D_y = 1 with different α (Table 1). Thus, when α = 1, the lateral buckling mode function $g(y)$ can be written as

$$g(y)=\left[\sin\left(\frac{\pi y}{b}\right)+0.0683\sin\left(\frac{2\pi y}{b}\right)\right] \quad (18)$$

In this study, only three cases are considered, i.e., α = 0, 1 and 2. For r = 0 and α = 1, C_1 = 1 and the C_2 value can be obtained from the following equation

$$C_2=0.1084-0.0566\left(\frac{D_x}{D_y}\right)^{0.25}+0.0168\left(\frac{D_x}{D_y}\right)^{0.5}-0.0005\frac{D_x}{D_y} \quad (19)$$

For Case III α = 2, the load is pure bending, and three terms in $g_i(y)$ need to be considered to obtain a more accurate result

$$g(y)=C_1\sin\left(\frac{\pi y}{b}\right)+C_2\sin\left(\frac{2\pi y}{b}\right)+C_3\sin\left(\frac{3\pi y}{b}\right) \quad (20)$$

The function $g_3(y)$ should satisfy (Harris and Piersol 2002)

$$g_3(0)=g_3\left(\frac{b}{3}\right)=g_3\left(\frac{2b}{3}\right)=g_3(b)=0 \quad (21a)$$

$$g_3''(0)=g_3''(b)=0 \quad (21b)$$

Similar to Case II, we can obtain

$$BC=0 \quad (22a)$$

where

$$B=\begin{bmatrix}\left(\frac{D_x}{D_y}+\phi^4+2\phi^2\right) & -\frac{32}{9\pi^2}K\phi^2 & 0\\ -\frac{32}{9\pi^2}K\phi^2 & \left(\frac{D_x}{D_y}+16\phi^4+8\phi^2\right) & -\frac{96}{25\pi^2}K\phi^2\\ 0 & -\frac{96}{25\pi^2}K\phi^2 & \left(\frac{D_x}{D_y}+81\phi^4+18\phi^2\right)\end{bmatrix} \quad (22b)$$

$$C=\begin{bmatrix}C_1\\C_2\\C_3\end{bmatrix} \quad (22c)$$

Table 1 Value of C_i (i = 1, 2 and 3)

Value of C_i	α								
	0	0.25	0.5	0.75	1	1.25	1.5	1.75	2
K_{cr0} from two-term approximation	4.000	4.569	5.319	6.344	7.810	10.010	13.397	18.343	24.982
K_{cr0} from three-term approximation	4.000	4.569	5.319	6.344	7.810	10.006	13.378	18.160	23.920
C_1	1	1	1	1	1	1	1	1	1
C_2	-	0.0098	0.0229	0.0411	0.0683	0.113	0.193	0.332	0.540
C_3	-	-	-	-	-	-	-	-	0.0882

The determinant of matrix B (here r = 0) has to be zero to obtain a non-trivial solution to Eq. (22). The value of K is a function of α and ϕ. Normally, if the value of α is given, the minimum value of K_{cr0} may be obtained. If α=2, C_1 is assumed as 1, so C_2 and C_3 can be evaluated according to Eq. (22). $g_i(y)$can be expressed in Eq. (23).

$$g(y) = \sin\left(\frac{\pi y}{b}\right) + 0.540\sin\left(\frac{2\pi y}{b}\right) + 0.0882\sin\left(\frac{3\pi y}{b}\right) \tag{23}$$

For r= 0 and α = 2, C_1 = 1, C_2 and C_3 values can be obtained from the following equations

$$C_2 = 0.5347 + 0.0097\left(\frac{D_x}{D_y}\right)^{0.5} - 0.0040\frac{D_x}{D_y} - 0.0002\left(\frac{D_x}{D_y}\right)^{1.5} + 0.0010\frac{D_x}{D_y}ln\left(\frac{D_x}{D_y}\right) \tag{24a}$$

$$C_3 = 0.1187 - 0.0431\left(\frac{D_x}{D_y}\right)^{0.25} + 0.0128\left(\frac{D_x}{D_y}\right)^{0.5} - 0.0004\frac{D_x}{D_y} \tag{24b}$$

From Table 1, it can be seen that the values of K_{cr} are close to each other between the two-term approximation and the three-term approximation except for α = 2. So for 0 < α < 2, the two-term approximation may be selected to satisfy the accuracy of results. For α = 2, the loading is pure bending, the three-term approximation has to be selected and there is only about 0.33% error between the three-term approximation and the four-term approximation (Timoshenko and Gere 1961).

The lateral buckling mode function $g(y)$ is plotted in Fig. 3 for α = 0, 1 and 2.

For α = 0, the loading is pure compression, substituting Eq. (12) into Eq. (9), the following equations can be derived

$$B_1 = 2\pi^2,\ B_2 = 1,\ B_3 = \pi^4,\ B_5 = 1 \quad \text{and} \quad \tilde{k}_2 = k_r = \frac{b^4 k_2}{\pi^4 D} \tag{5a2}$$

For α = 1, the loading is a triangular distribution compressive loading, substituting Eq. (14) into Eq. (8) yields

$$B_1 = 2\pi^2\frac{(1+4C_2^2)}{1+C_2^2},\ B_2 = \left[\frac{9\pi^2(1+C_2^2)+64C_2}{18\pi^2(1+C_2^2)}\right],\ B_3 = \pi^4\frac{1+16C_2^2}{1+C_2^2},\ B_5 = \frac{1+C_2^2}{1+16C_2^2} \quad \text{and} \quad \tilde{k}_2 = k_r = \frac{b^4 k_2}{\pi^4 D} \tag{25b}$$

where C_2 = 0.0683 can be obtained by using Eq. (19) with D_x/D_y = 1 .

For α = 2, the loading is pure bending, substituting Eq. (20) into Eq. (8) yields

$$B_1 = 2\pi^2\frac{(1+4C_2^2+9C_3^2)}{1+C_2^2+C_3^2},\ B_2 = \left[\frac{64C_2}{9\pi^2(1+C_2^2+C_3^2)} + \frac{192C_2C_3}{25\pi^2(1+C_2^2+C_3^2)}\right],\ B_3 = \pi^4\frac{1+16C_2^2+81C_3^2}{1+C_2^2+C_3^2},\ B_5 = \frac{1+C_2^2+C_3^2}{1+16C_2^2+81C_3^2} \quad \text{and} \quad \tilde{k}_2 = k_r = \frac{b^4 k_2}{\pi^4 D} \tag{25c}$$

where C_2 and C_3 can be calculated by using Eq. (24). If D_x/D_y = 1, C_2 = 0.540 and C_3 = 0.0882.

2.2.2 Clamped support

For two unloaded edges clamped, the lateral buckling mode function of an infinitely long plate can be considered as (Blevins 2015)

$$g_i(y) = \cosh\left(\frac{p_i}{b}y\right) - \cos\left(\frac{p_i}{b}y\right) - q_i\left[\sinh\left(\frac{p_i}{b}y\right) - \sin\left(\frac{p_i}{b}y\right)\right] \tag{26}$$

where

$$\cos p_i \cosh p_i = 1 \tag{27a}$$

$$q_i = \frac{\cosh p_i - \cos p_i}{\sinh p_i - \sin p_i} \tag{27b}$$

where p_i and q_i can be obtained from (Blevins 2015)

For case I: 0 ≤ α < 2, (it is noted that only two cases are considered for this boundary condition) to get more accurate results, three terms of $g_i(y)$ are considered, the function and the first derivative of $g_i(y)$ (i = 1, 2 and 3) should satisfy (Harris and Piersol 2002)

$$g_1(0) = g_1(b) = 0 \tag{28a}$$

$$g_2(0) = g_2\left(\frac{b}{2}\right) = g_2(b) = 0 \tag{28b}$$

$$g_3(0) = g_3(0.359\text{b}) = g_3(0.641\text{b}) = g_3(b) = 0 \tag{28c}$$

$$g_i'(0) = g_i'(b) = 0 \quad (i = 1, 2 \text{ and } 3) \tag{28d}$$

$$g(y) = C_1 g_1 + C_2 g_2 + C_3 g_3 \tag{28e}$$

Thus, Eq. (29) can be obtained

$$\mathbf{BC} = 0 \tag{29a}$$

where

$$\mathbf{B} = \begin{bmatrix} d_1 - K\phi^2 2\left(1-\frac{\alpha}{2}\right) & K\phi^2 d_4 & d_5 \\ K\phi^2 d_4 & d_2 - K\phi^2 2\left(1-\frac{\alpha}{2}\right) & K\phi^2 d_6 \\ d_5 & K\phi^2 d_6 & d_3 - K\phi^2 2\left(1-\frac{\alpha}{2}\right) \end{bmatrix} \tag{29b}$$

$$\mathbf{C} = \begin{bmatrix} C_1 \\ C_2 \\ C_3 \end{bmatrix} \tag{29c}$$

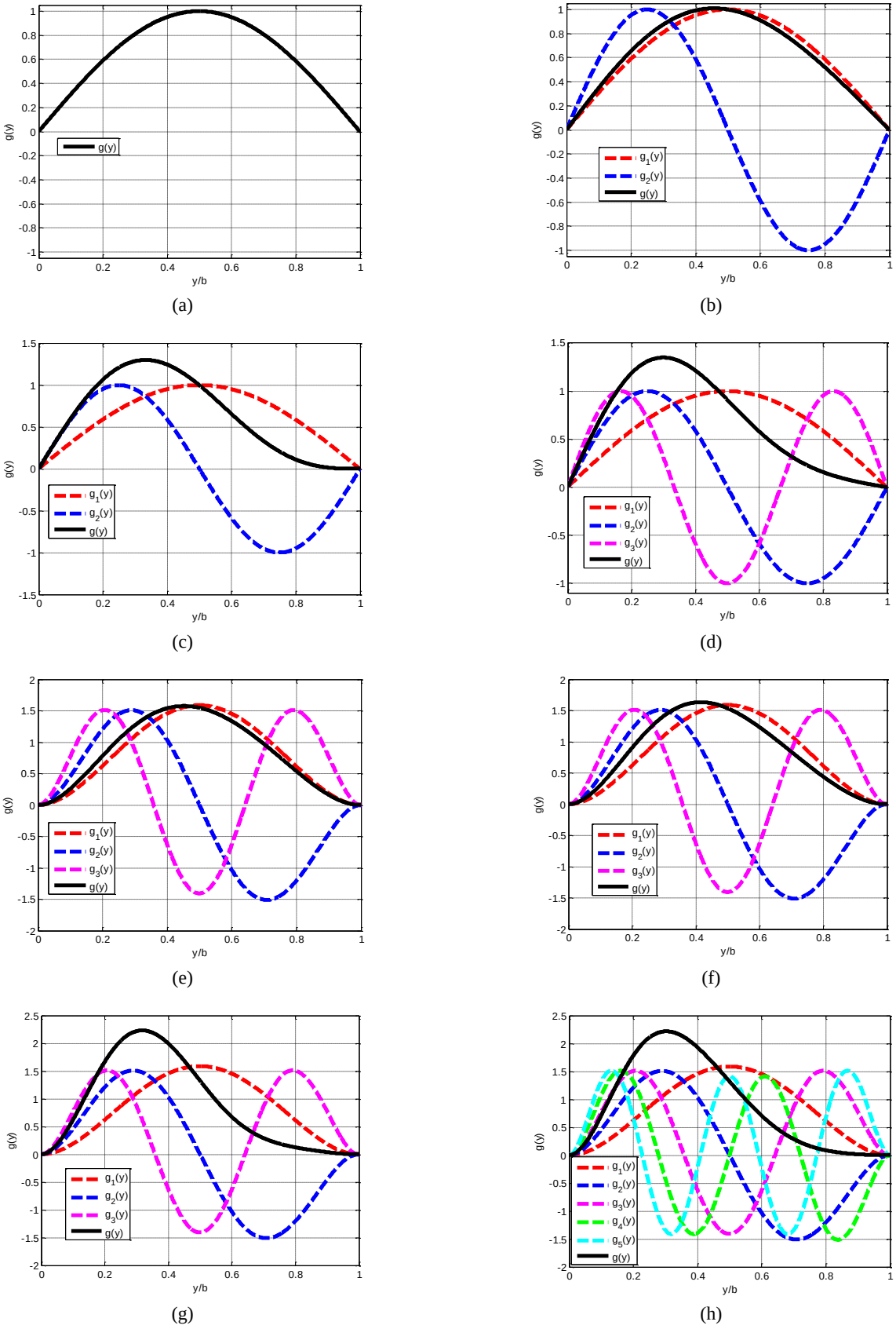

Fig. 3 Lateral buckling mode function $g(y)$, (a) the one-term approximation for simply supported edges ($\alpha = 0$); (b) the two-term approximation for simply supported edges ($\alpha = 1$); (c) the three-term approximation for simply supported edges ($\alpha = 2$); (e) the three-term approximation for clamped edges ($\alpha = 0$); (f) the three-term approximation for clamped edges ($\alpha = 1$); (g) the three-term approximation for clamped edges ($\alpha = 2$); (h) the five-term approximation for clamped edges ($\alpha = 2$)

where the values for d_i are defined as $d_i = 2\frac{D_x}{D_y} + 2\frac{\phi^4}{\pi^4}{p_i}^4 - 4\frac{\mathrm{H}}{D_y}\frac{\phi^2}{\pi^2}p_i q_i(2 - p_i q_i), (i = 1,2,3);\ d_4 = -64\alpha\frac{{p_1}^3{p_2}^3 q_1 q_2}{({p_1}^4 - {p_2}^4)^2};$

$d_5 = 32\frac{\mathrm{H}}{D_y}\frac{\phi^2}{\pi^2}\frac{{p_1}^2{p_3}^2(p_1 q_1 - p_3 q_3)}{{p_1}^4 - {p_3}^4}$ and $d_6 = -64\alpha\frac{{p_3}^3{p_2}^3 q_3 q_2}{({p_3}^4 - {p_2}^4)^2}.$

The value of K is a function of α and ϕ. Once the value of α is given, the minimum value of K_{cr0} may be obtained (r = 0). For example, when D_x/D_y = 1, α = 0 and α = 1, according to Eq. (29) C_i values can be obtained as in Table 2 with the lateral buckling mode function as in Eqs. (30a) and (30b), respectively.

$$g(y) = g_1(y) + 0.0244 g_3(y) \tag{30a}$$

$$g(y) = g_1(y) + 0.0965\, g_2(y) + 0.0278 g_3(y) \tag{30b}$$

Similarly, only three cases are considered, i.e., α = 0, 1 and 2. For r = 0 and α = 0, C_1 = 1, C_2 = 0 and the C_3 value can be obtained from the following equation

$$C_3 = 0.0784 - 0.0774\left(\frac{D_x}{D_y}\right)^{0.25} + 0.0239\left(\frac{D_x}{D_y}\right)^{0.5} - 0.0008\frac{D_x}{D_y} \tag{31}$$

For r = 0 and α = 1, C_1 = 1, C_2 and C_3 value can be obtained from the following equations

$$C_2 = 0.1109 - 0.0201\left(\frac{D_x}{D_y}\right)^{0.25} + 0.0059\left(\frac{D_x}{D_y}\right)^{0.5} - 0.0002\frac{D_x}{D_y} \tag{32a}$$

$$C_3 = 0.0839 - 0.0804\left(\frac{D_x}{D_y}\right)^{0.25} + 0.0248\left(\frac{D_x}{D_y}\right)^{0.5} - 0.0008\frac{D_x}{D_y} \tag{32b}$$

Case II α = 2, the load is pure bending, n can be selected as 5 for obtaining more accurate results

$$g(y) = C_1 g_1(y) + C_2 g_2(y) + C_3 g_3(y) + C_4 g_4(y) + C_5 g_5(y) \tag{33}$$

The function and the first derivative of $g_4(y)$ and $g_5(y)$ should satisfy (Harris and Piersol 2002)

$$g_4(0) = g_4(0.278\mathrm{b}) = g_4(0.5\mathrm{b}) = g_4(0.722\mathrm{b}) = g_4(b) = 0 \tag{34a}$$

$$g_5(0) = g_5(0.227\mathrm{b}) = g_5(0.409\mathrm{b}) = g_5(0.591\mathrm{b}) = g_5(0.773\mathrm{b}) = g_5(b) = 0 \tag{34b}$$

$$g_4{}'(0) = g_4{}'(b) = g_5{}'(0) = g_5{}'(b) = 0 \tag{34c}$$

Eq. (34) may be rewritten in matrix form as

$$\mathbf{BC} = 0 \tag{35a}$$

$$\mathbf{B} = \begin{bmatrix} d_1 & K\varphi^2 d_6 & d_7 & K\varphi^2 d_8 & d_9 \\ & d_2 & K\varphi^2 d_{10} & d_{11} & K\varphi^2 d_{12} \\ & & d_3 & K\varphi^2 d_{13} & d_{14} \\ & & & d_4 & K\varphi^2 d_{15} \\ & & & & d_5 \end{bmatrix} \tag{35b}$$

$$\mathbf{C} = [C_1\ \ C_2\ \ C_3\ \ C_4\ \ C_5]^T \tag{35c}$$

where B in Eq. (35) is a symmetric matrix and the values of d_i can be defined as

$$d_i = 2\frac{D_x}{D_y} + 2\frac{\phi^4}{\pi^4}{p_i}^4 - 4\frac{\mathrm{H}}{D_y}\frac{\phi^2}{\pi^2}p_i q_i(2 - p_i q_i), \quad (i = 1,2,3,4,5);$$

Table 2 Value of C_i (i = 1, 2, 3, 4 and 5)

Value of C_i	α								
	0	0.25	0.5	0.75	1	1.25	1.5	1.75	2
K_{cr0} from 2nd approximation	7.027	8.026	9.340	11.131	13.678	17.463	23.245	31.976	45.228
K_{cr0} from 3rd approximation	6.979	7.971	9.275	11.049	13.564	17.270	22.798	30.528	40.241
K_{cr0} from 4th approximation	6.979	7.971	9.275	11.049	13.562	17.264	22.773	30.429	39.826/ 39.631*
C_1	1	1	1	1	1	1	1	1	1
C_2	0	0.014	0.0326	0.0583	0.0965	0.157	0.261	0.430	0.652
C_3	0.0244	0.0244	0.0247	0.0256	0.0278	0.0335	0.0497	0.0943	0.204
C_4	0	0	0	0	0	0	0	0	0.0456
C_5	0	0	0	0	0	0	0	0	0.0145

* from 5th approximation

$$d_6 = -64\alpha \frac{{p_1}^3 {p_2}^3 q_1 q_2}{({p_1}^4 - {p_2}^4)^2};$$

$$d_7 = -32 \frac{\mathrm{H}}{D_y} \frac{\phi^2}{\pi^2} \frac{{p_1}^2 {p_3}^2 (p_1 q_1 - p_3 q_3)}{{p_1}^4 - {p_3}^4};$$

$$d_8 = -64\alpha \frac{{p_1}^3 {p_4}^3 q_1 q_4}{({p_1}^4 - {p_4}^4)^2};$$

$$d_9 = -32 \frac{\mathrm{H}}{D_y} \frac{\phi^2}{\pi^2} \frac{{p_1}^2 {p_5}^2 (p_1 q_1 - p_5 q_5)}{{p_1}^4 - {p_5}^4};$$

$$d_{10} = -64\alpha \frac{{p_3}^3 {p_2}^3 q_3 q_2}{({p_3}^4 - {p_2}^4)^2};$$

$$d_{11} = -32 \frac{\mathrm{H}}{D_y} \frac{\phi^2}{\pi^2} \frac{{p_2}^2 {p_4}^2 (p_2 q_2 - p_4 q_4)}{{p_2}^4 - {p_4}^4};$$

$$d_{12} = -64\alpha \frac{{p_2}^3 {p_5}^3 q_2 q_5}{({p_2}^4 - {p_5}^4)^2};$$

$$d_{13} = -64\alpha \frac{{p_3}^3 {p_4}^3 q_3 q_4}{({p_3}^4 - {p_4}^4)^2};$$

$$d_{14} = -32 \frac{\mathrm{H}}{D_y} \frac{\phi^2}{\pi^2} \frac{{p_3}^2 {p_5}^2 (p_3 q_3 - p_5 q_5)}{{p_3}^4 - {p_5}^4};$$

and $$d_{15} = -64\alpha \frac{{p_5}^3 {p_4}^3 q_5 q_4}{({p_5}^4 - {p_4}^4)^2}.$$

The value of K is a function of α and ϕ. Once the value of α is given, the minimum value of K_{cr0} may be obtained (r = 0). If D_x/D_y = 1 and α = 2, the lateral buckling function can be obtained

$$g(y) = g_1(y) + 0.653 g_2(y) + 0.204 g_3(y)) + 0.0456 g_4(y) + 0.0145 g_5(y) \quad (36)$$

For r = 0 and α = 2, C_1 = 1, C_2, C_3, C_4 and C_5 values can be obtain from the following equations

$$C_2 = 0.5525 + 0.1386 \left(\frac{D_x}{D_y}\right)^{0.25} - 0.0386 \left(\frac{D_x}{D_y}\right)^{0.5} - 0.0011 \frac{D_x}{D_y} \quad (37a)$$

$$C_3 = 0.2567 - 0.0758 \left(\frac{D_x}{D_y}\right)^{0.25} + 0.0231 \left(\frac{D_x}{D_y}\right)^{0.5} - 0.0007 \frac{D_x}{D_y} \quad (37b)$$

$$C_4 = 0.0945 - 0.0694 \left(\frac{D_x}{D_y}\right)^{0.25} + 0.0210 \left(\frac{D_x}{D_y}\right)^{0.5} - 0.0006 \frac{D_x}{D_y} \quad (37c)$$

$$C_5 = 0.0412 - 0.0384 \left(\frac{D_x}{D_y}\right)^{0.25} + 0.0120 \left(\frac{D_x}{D_y}\right)^{0.5} - 0.0004 \frac{D_x}{D_y} \quad (37d)$$

For $0 \le \alpha < 2$, the three-term approximation may be selected to provide sufficiently accurate results. For example, if α = 0, the results are 7.027, 6.979 and 6.979 for the two-term approximation, and the three-term approximation and the four-term approximation, respectively. The results for α = 1 are 13.678, 13.564 and 13.562, respectively. The differences are within 1% between the two-term approximation and the three-term approximation. There is nearly no change between the three-term approximation results and the four-term approximation. Thus, the three-term approximation is enough for cases with $0 \le \alpha < 2$. For α = 2, the pure bending case, the five-term approximation has to be selected for the lateral buckling mode. The results for buckling coefficient are 40.241, 39.826 and 39.631 for the three-term approximation, four-term approximation and five-term approximation, respectively. The differences are ~0.49% between the four-term-approximation and the five-term approximation. The lateral buckling mode function $g(y)$ is plotted in Fig. 3 for α = 0, 1 and 2.

Thus, for α = 0 or α = 1, the loading is compression, substituting Eq. (28e) into Eq. (8), we have

$$\begin{aligned} B_1 &= \frac{2p_1 q_1 (p_1 q_1 - 2) + 2C_2^2 p_2 q_2 (p_2 q_2 - 2) + 2C_3^2 p_3 q_3 (p_3 q_3 - 2)}{1 + C_2^2 + C_3^2} \\ &\quad -32 C_3 \frac{p_1^2 p_3^2 (p_1 q_1 - p_3 q_3)}{(1 + C_2^2 + C_3^2)(p_1^4 - p_3^4)}, \\ B_2 &= \left[1 - \frac{\alpha}{2} + 64\alpha C_2 \frac{p_1^3 p_2^3 q_1 q_2}{(1 + C_2^2 + C_3^2)(p_1^4 - p_2^4)^2} \right. \\ &\quad \left. +64\alpha C_2 C_3 \frac{p_3^3 p_2^3 q_3 q_2}{(1 + C_2^2 + C_3^2)(p_3^4 - p_2^4)^2}\right] \\ B_3 &= \frac{p_1^4 + C_2^2 p_2^4 + C_3^2 p_3^4}{1 + C_2^2 + C_3^2}, \\ B_5 &= \frac{p_1^4}{B_3} \quad \text{and} \quad \tilde{k}_2 = k_r = \frac{b^4 k_2}{p_1^4 D_y} \end{aligned} \quad (38)$$

where p_i and q_i can be obtained in (Blevins 2015); C_2 and C_3 can be calculated by using Eqs. (31) and (32) for α = 0 and α = 1, respectively. Specifically, for D_x/D_y = 1 and α = 0, C_2 = 0 and C_3 = 0.0244; for D_x/D_y = 1 and α = 1, C_2 = 0.0965 and C_3 = 0.0278.

For α = 2, the loading is pure bending, substituting Eq. (33), Eq. (8), we obtain

$$B_1 = \sum_{i=1}^{5} \left[\frac{2C_i^2 p_i q_i (p_i q_i - 2)}{\sum_{m=1}^{5} C_m^2}\right] - 32 \sum_{i,j=1}^{5(i+j=even)} \left[\frac{C_i C_j p_i^2 p_j^2 (p_i q_i - p_j q_j)}{(p_i^4 - p_j^4) \sum_{m=1}^{5} C_m^2}\right], \quad (39)$$

$$B_2 = 128 \sum_{i,j=1}^{5(i+j=odd)} \left[\frac{C_i C_j p_i^3 p_j^3 q_i q_j}{(p_i^4 - p_j^4)^2 \sum_{m=1}^{5} C_m^2}\right],$$

$$B_3 = \sum_{i=1}^{5}\left(\frac{C_i^2 p_i^4}{\sum_{m=1}^{5} C_m^2}\right), \quad B_5 = \frac{p_1^4}{B_3} \quad \text{and} \quad \tilde{k}_2 = k_r = \frac{b^4 k_2}{p_1^4 D_y} \tag{39}$$

where p_i and q_i (i = 1, 2, 3, 4 and 5) can be obtained from (Blevins 2015); C_1 = 1 and C_i (i = 2, 3, 4 and 5) can be calculated by using Eq. (37). If D_x/D_y = 1, C_1 = 1, C_2 = 0.653, C_3 = 0.204, C_4 = 0.0456 and C_5 = 0.0145.

2.3 Solutions

The symmetric solution of Eq. (9) may be written as

$$\tilde{f}_i(\xi_i) = A_{i1} f_{i1} + A_{i2} f_{i2} \tag{40}$$

where A_{i1} and A_{i2} are the unknown coefficients to be determined and depend on the value of

$$\Delta_i = \frac{(B_1(1+r) - B_2\pi^2 K)^2}{4} - B_3 \frac{D_x}{D_y}\left(1 + B_5 \tilde{k}_i\right),$$

the functions f_{i1} and f_{i2} may be obtained from the following three cases.

Case 1: $\Delta_i > 0$

$$f_{i1}(\xi_i) = \cos(\alpha_i \xi_i) \tag{41a}$$

$$f_{i2}(\xi_i) = \cos(\beta_i \xi_i) \tag{41b}$$

$$\alpha_i, \beta_i = \frac{\gamma_i}{\sqrt{D_x/D_y}} \sqrt{\frac{B_1(1+r) - B_2\pi^2 K}{2} \pm \sqrt{\Delta_i}} \tag{41c}$$

Case 2: $\Delta_i = 0$

$$f_{i1}(\xi_i) = \cos(\alpha_i \xi_i) \tag{42a}$$

$$f_{i2}(\xi_i) = \xi_i \sin(\alpha_i \xi_i) \tag{42b}$$

$$\alpha_i = \frac{\gamma_i}{\sqrt{D_x/D_y}} \sqrt{\frac{B_1(1+r) - B_2\pi^2 K}{2}} \tag{42c}$$

Case 3: $\Delta_i < 0$

$$f_{i1}(\xi_i) = \cosh(\alpha_i \xi_i)\cos(\beta_i \xi_i) \tag{43a}$$

$$f_{i2}(\xi_i) = \sinh(\alpha_i \xi_i)\sin(\beta_i \xi_i) \tag{43b}$$

$$\alpha_i,\ \beta_i = \frac{\gamma_i}{\sqrt{D_x/D_y}} \sqrt{\sqrt{\left(\frac{B_1(1+r) - B_2\pi^2 K}{2}\right)^2 - \Delta_i} \mp \left(\frac{B_1(1+r) - B_2\pi^2 K}{2}\right)} \tag{43c}$$

2.4 Continuity condition

Considering that the displacement on the borderline separating the contact and non-contact areas must be zero, additional equations need to be satisfied

$$\tilde{f}_1\left(\frac{-1}{2}\right) = A_{11} f_{11}\left(\frac{-1}{2}\right) + A_{12} f_{12}\left(\frac{-1}{2}\right) = 0 \tag{44a}$$

$$\tilde{f}_2\left(\frac{1}{2}\right) = A_{21} f_{21}\left(\frac{1}{2}\right) + A_{22} f_{22}\left(\frac{1}{2}\right) = 0 \tag{44b}$$

The continuity condition between f_1 and f_2 is

$$f_1'\left(\frac{-a_1}{2}\right) = f_2'\left(\frac{a_2}{2}\right) \tag{45a}$$

$$f_1''\left(\frac{-a_1}{2}\right) = f_2''\left(\frac{a_2}{2}\right) \tag{45b}$$

$$f_1'''\left(\frac{-a_1}{2}\right) = f_2'''\left(\frac{a_2}{2}\right) \tag{45c}$$

Table 3 Values of λ_i (i = 1 and 2)

α value	Boundary condition	λ_i	k_r						
			$\leq 10^{-3}$	10^{-2}	10^{-1}	10^{0}	10^{1}	10^{2}	$\geq 10^{3}$
0	CC	λ_1	4.577	4.598	4.791	6.439	6.933	7.542	7.619
		λ_2	2.402	2.403	2.408	2.407	2.407	2.405	2.408
	SS	λ_1	2.000	2.010	2.098	2.828	3.042	3.318	3.333
		λ_2	1.999	2.000	2.000	2.000	1.977	1.997	2.000
1	CC	λ_1	8.914	8.955	9.316	12.363	13.763	14.445	14.856
		λ_2	4.650	4.650	4.651	4.651	4.656	4.537	4.650
	SS	λ_1	3.944	3.962	4.124	5.486	6.120	6.405	6.573
		λ_2	3.866	3.867	3.866	3.866	3.846	3.860	3.866
2	CC	λ_1	26.739	26.774	27.085	30.013	36.058	43.452	44.566
		λ_2	12.892	12.891	12.891	12.891	13.568	13.535	12.891
	SS	λ_1	13.424	13.438	13.562	14.744	18.004	21.817	22.373
		λ_2	10.496	10.496	10.496	10.496	10.467	10.552	10.496

*Note: SS-simply supported; CC-clamped

3. Results verification

Solving Eqs. (44) and (45), the values of K may be obtained. The K value is a function expressed in terms of a_1, a_2. The minimum value of K is the buckling coefficient K_{cr} which is a function of coefficients r, k_r and D_x/D_y. In order to obtain the solution easily, ignoring the influence of coefficient r (i.e., assuming H/D_y = 1, or r = 0), and considering k_r to be a constant, the buckling coefficient K_{cr0} (r = 0) is only a function of D_x/D_y. In other words, if the k_r value is constant, K_{cr0} (r = 0) may be obtained for various D_x/D_y values. Thus, based on the analytical solution of K_{cr0} and D_x/D_y for each k_r value, the relationship between the buckling coefficient K_{cr0} and the flexural rigidity ratio of D_x/D_y can be obtained. Hence, a fitted formula for K_{cr0} (r = 0) can be developed as follows

$$K_{cr0} = \lambda_1 \left(\frac{D_x}{D_y}\right)^{0.5} + \lambda_2 \tag{46}$$

where the values of λ_i (i = 1 and 2) may be obtained directly from Table 3 (based on k_r).

The variation trend of the ratio of buckling coefficient (between $k_r \geq 1000$ and $k_r \leq 0.001$) for the different loading parameters α can be found in Fig. 4. For an isotropic plate under pure compression (α = 0), Fig. 4 shows that the difference of buckling coefficients between $k_r \geq 1000$ and $k_r \leq 0.001$ is ~33.333% and ~43.670 % for simply supported plates and clamped plates, respectively. The results are close to previous studies of ~33% in (Seide 1958) and ~43.41% in (Ma *et al*. 2008a).

The above solutions are based on the assumption of r = 0, and assuming the governing equation (r = 0) has the same lateral buckling mode function with the governing equation ($r \neq 0$), where the governing equations are modifications from Eq. (9)

$$\frac{D_x}{D_y}\tilde{f}_i''''(\xi_i) - \gamma_i{}^2[B_1 - \pi^2 K_{cr0} B_2]\tilde{f}_i''(\xi_i) + B_3\gamma_i{}^4(1 + B_5 k_i)\tilde{f}_i(\xi_i) = 0 \tag{47}$$

To include the influence of r, the final bucking coefficient K_{cr} may be obtained by subtracting Eq. (47) from Eq. (9)

$$K_{cr} = K_{cr0} + \frac{B_1 r}{B_2 \pi^2} \tag{48}$$

in which B_1 and B_2 may be determined using Eqs. (25), (38) and (39). For example, if D_x/D_y = 1, α = 0 and the boundary condition is clamped, according to Eq. (38), B_1 = 23.760 and B_2 = 1.000, thus Eq. (48) can be rewritten as $K_{cr} = K_{cr0} + 23.76\frac{r}{\pi^2}$.

To further validate the proposed solutions, the flat plate (i.e., H/D_y = 1, D_x/D_y = 1) without foundation (i.e., foundation stiffness factor k_r = 0) is taken into account

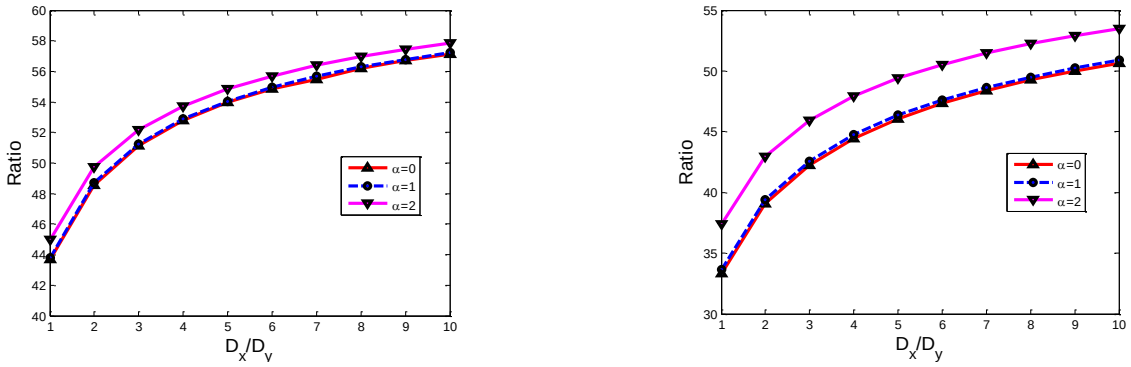

(a) (b)

Fig. 4 Critical buckling coefficient ratio between foundation parameters k_r = 1000 and k_r = 0.001; (a) clamped and (b) simply supported

Table 4 Comparison of buckling coefficients when k_r = 0

Value of α	Cond.	Present study	Previous study						
			(Timoshenko and Gere 1961)	(Nölke 1937)	(Bulson 1970)	(Leissa and Kang 2002, Kang and Leissa 2005)	(Weaver and Nemeth 2007)	(Tarján *et al.* 2009)	(Liu *et al.* 2014)
α = 0	CC	6.979			6.97	6.97	6.95	6.97	6.98
	SS	4.000	4.0		4.0	4.0	4.0	4.0	4.0
α = 1	CC	13.564		13.56	13.56	13.55			
	SS	7.810	7.8		7.81	7.81			
α = 2	CC	39.631		39.61	39.61	39.56	39.46	39.70	39.55
	SS	23.920	23.9		23.9	23.88	23.87	23.8	23.912

(Table 4). For the foundation stiffness factor k_r = 0, the current solutions are compared with the previously published results (Timoshenko and Gere 1961, Bulson 1970, Nölke 1937, Leissa and Kang 2002, Kang and Leissa 2005, Weaver and Nemeth 2007, Tarján *et al*. 2009, Liu *et al*. 2014). Timoshenko and Gere (1961) presented the buckling coefficients of a simply supported plate using the energy method for α = 0, α = 1 and α = 2. Nölke (1937) illustrated the buckling coefficients of a clamped plate using the energy method for α = 1 and α = 2. Bulson (1970) summarized the buckling coefficients of square plates with both clamped and simply supported edges for α = 0, α = 1 and α = 2. The exact solutions of the plate were obtained using the power series method for α = 0, α = 1 and α = 2 (Leissa and Kang 2002, Kang and Leissa 2005). For α = 0 and α = 2, the buckling coefficients of the composite plate with both clamped and simply supported edges were analysed (isotropic plate was the special case) (Weaver and Nemeth 2007, Tarján *et al*. 2009, Liu *et al*. 2014). As shown in Table 4, good agreement was obtained between the current method and the previous studies.

4. Numerical examples and discussion

4.1 Example 1

A corrugated thin plate with triangle shape is considered, as presented in Fig. 5. In this example, the material properties for the steel plate were: E^s = 205 GPa (elastic modulus), v^s = 0.3 (Poisson's ratio). The dimensions of the steel plate were t = 1 mm (plate thickness), l = 2000 mm (plate length), b = 200 mm (plate width) and h = 1, 2 and 3 mm. The clamped boundary condition was considered in this example. The commercial software ABAQUS was used to perform the buckling simulation of the steel plate. In the FE analysis, the steel sheet profile was modelled according to its real geometry and the thin skin was represented as S4R elements. The elastic foundation was simulated through tensionless elastic springs.

The comparisons between the analytical critical stress and the FE results were plotted in Fig. 6. The height of the corrugated triangle varied between 1 and 3 mm. Three kinds of elastic foundation were taken into account, i.e., k_r =

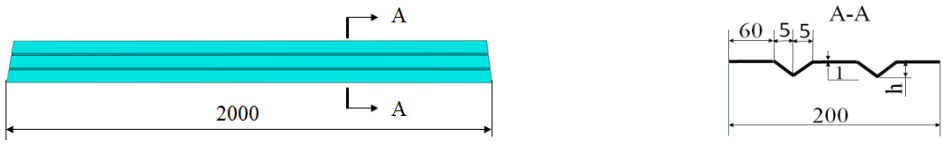

(a) (b)

Fig. 5 Sheet geometry: (a) corrugated sheet; and (b) cross-section

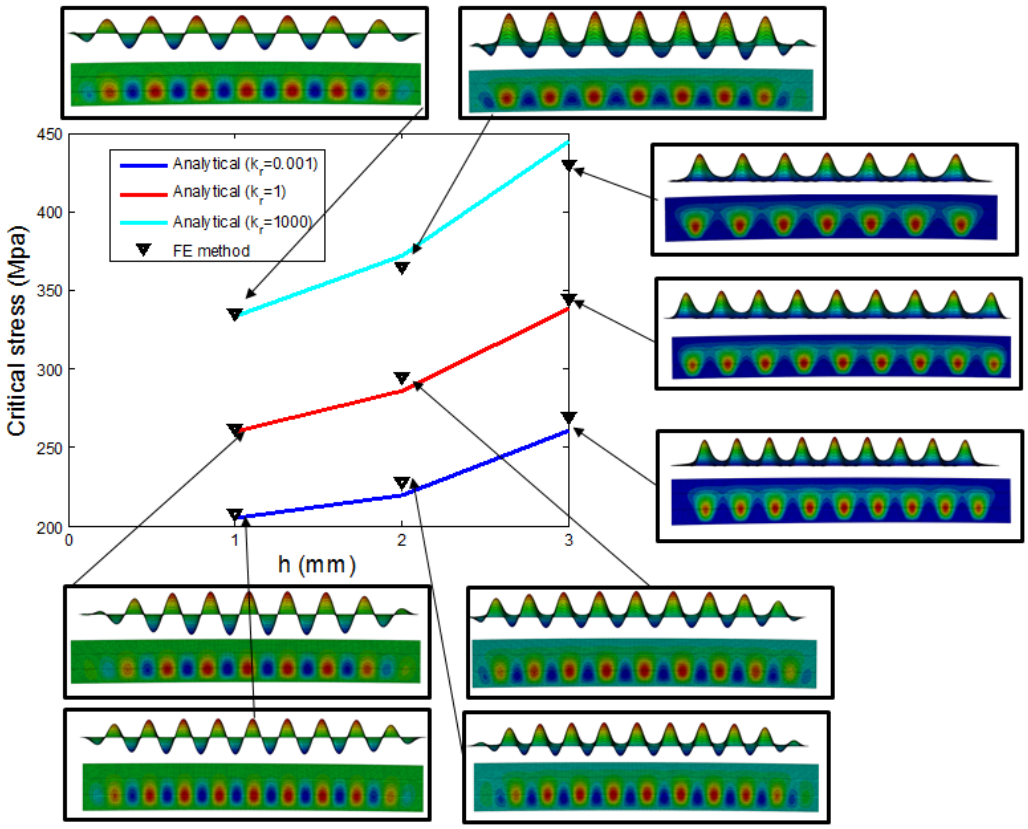

Fig. 6 Critical stresses for clamped corrugated skin sheets under pure bending

0.001, 1 and 1000. From Fig. 6, the discrepancy is not more than 5% between the current analytical solutions and the FE results.

4.2 Example 2

When $h = 0$ in example 1, the corrugated plate becomes a flat plate, so the flat plate (isotropic plate) can be regarded as a special case of the profiled plate. In this example, the material properties and dimensions of the steel plate are the same as example 1. Thus, according to Eq. (2), $D_x = D_y = H$ (i.e., $H/D_y = 1$, $D_x/D_y = 1$).

The critical buckling loads of a thin steel plate supported by a tensionless foundation under linearly varying in-plane loads were obtained by both analytical and fitted methods for $\alpha = 0$, $\alpha = 1$ and $\alpha = 2$. The buckling coefficients and related buckling modes in terms of varying foundation factors are shown in Figs. 7, 8, 9, respectively. Two boundary conditions (simply supported and clamped) are given. Three foundation factors $k_r = 0.001$, 1, 1000 are considered. Both analytical results and fitted formula results agree well with FEM simulations.

For practical applications, the stiffness parameters of corrugated plates can be determined through Eq. (2). The foundation factors k_r can be obtained through the material properties and geometry parameters of steel sheets and filler material (Ma *et al.* 2008a). Considering the loading parameter α and boundary conditions at lateral edges, the contact buckling coefficient of the system can be achieved through Eqs. (46) and (48) with calculation factors from Table 3.

4.3 Discussion

4.3.1 Effect of loading parameter α

Normally, $0 \le \alpha \le 2$ is taken into account in most studies. For $\alpha = 0$, the loading is considered as pure uniform axial compression. For $\alpha = 1$, the loading is a triangular distribution load. For $\alpha = 2$, the loading is regarded as pure bending. For $0 < \alpha < 1$, the load is non-uniform compressive loading. For $1 < \alpha < 2$, the load consists of compression and tension, i.e., compressive load on the bottom part and tensile load on the top part. From Fig. 8 ($\alpha = 0$), it demonstrates that the buckling mode shapes of the thin steel plate are symmetrical about the neutral axis $y = b/2$. This phenomenon is in accordance with the study of Leissa and Kang (2002). From Fig. 10 ($\alpha = 2$), it can be observed that the centre line of the buckling mode shape deviates from the mid-axis $y = b/2$ to the line $y = 0$. Generally, the centre line of the buckling mode shapes of the thin steel is between the mid-axis $y = b/2$ and $y = 0$. From Fig. 9 ($\alpha = 1$), the buckling mode shapes are similar to

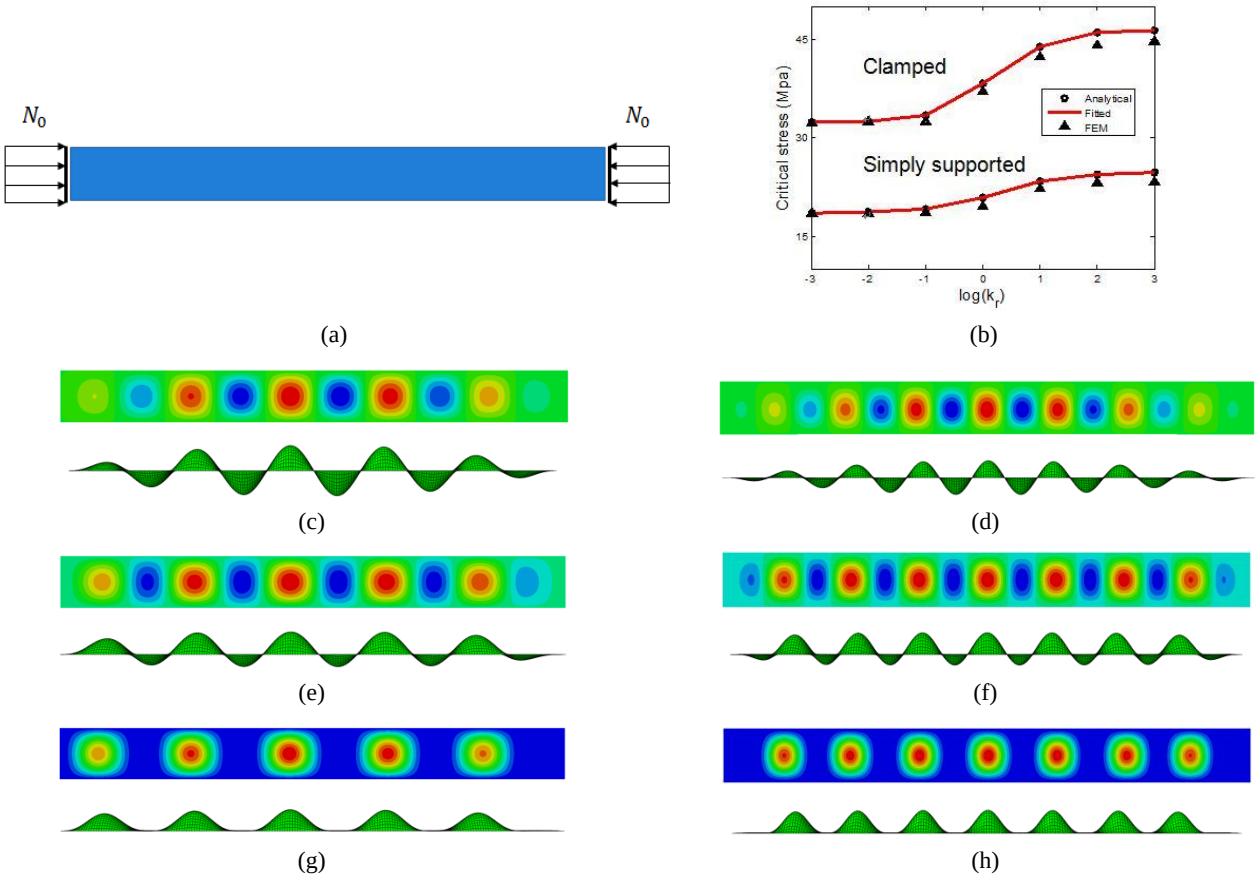

Fig. 7 Buckling coefficient and buckling model of a steel plate supported by foundation when $\alpha = 0$ (pure uniform compression), (a) loading mode; (b) buckling coefficients; (c) simply supported edges and $k_r = 0.001$; (d) clamped edges and $k_r = 0.001$; (e) simply supported edges and $k_r = 1$; (f) clamped edges and $k_r = 1$; (g) simply supported edges and $k_r = 1000$; and (h) clamped edges and $k_r = 1000$

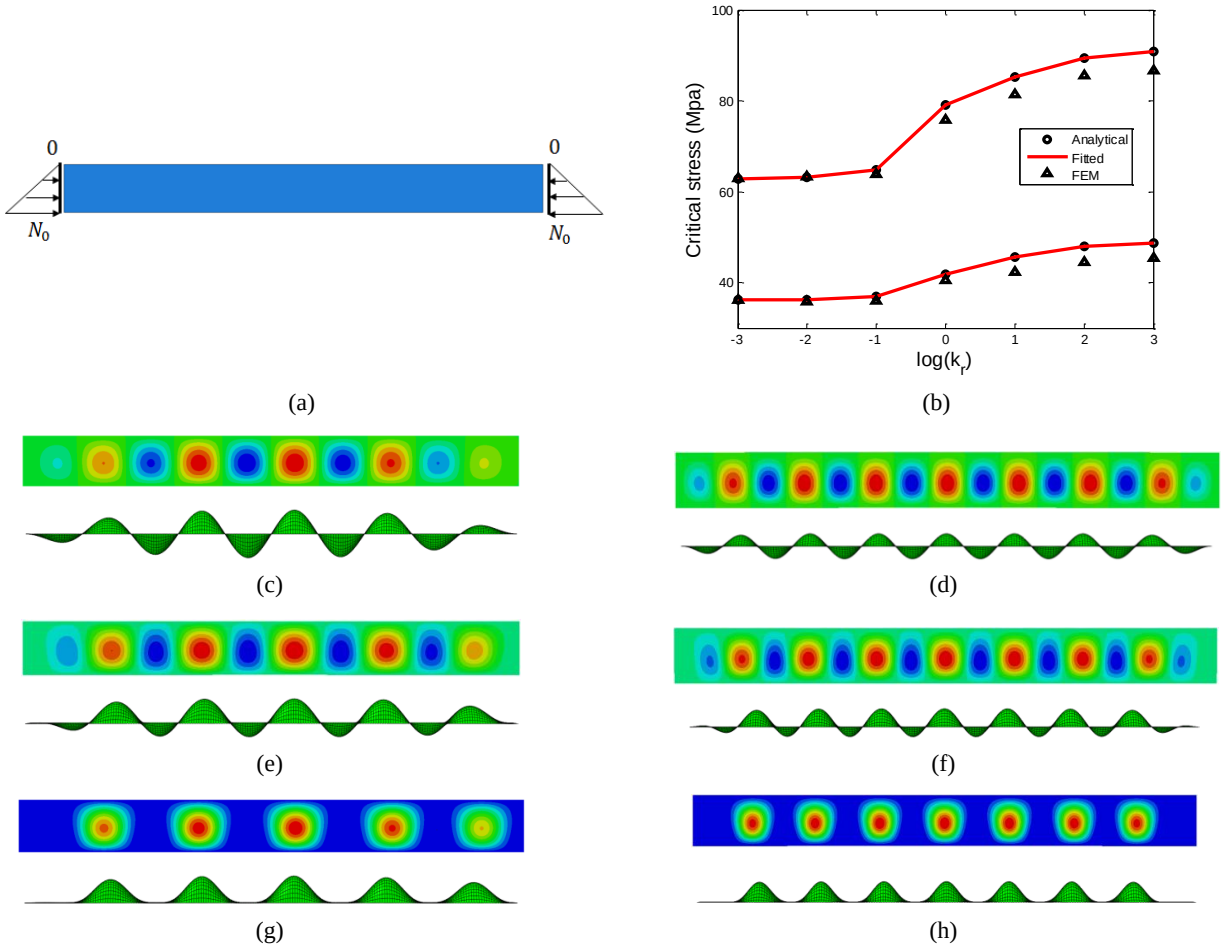

Fig. 8 Buckling coefficient and buckling model of a steel plate supported by foundation when α = 1, (a) loading mode; (b) buckling coefficients; (c) simply supported edges and k_r = 0.001; (d) clamped edges and k_r = 0.001; (e) simply supported edges and k_r = 1; (f) clamped edges and k_r = 1; (g) simply supported edges and k_r = 1000; and (h) clamped edges and k_r = 1000

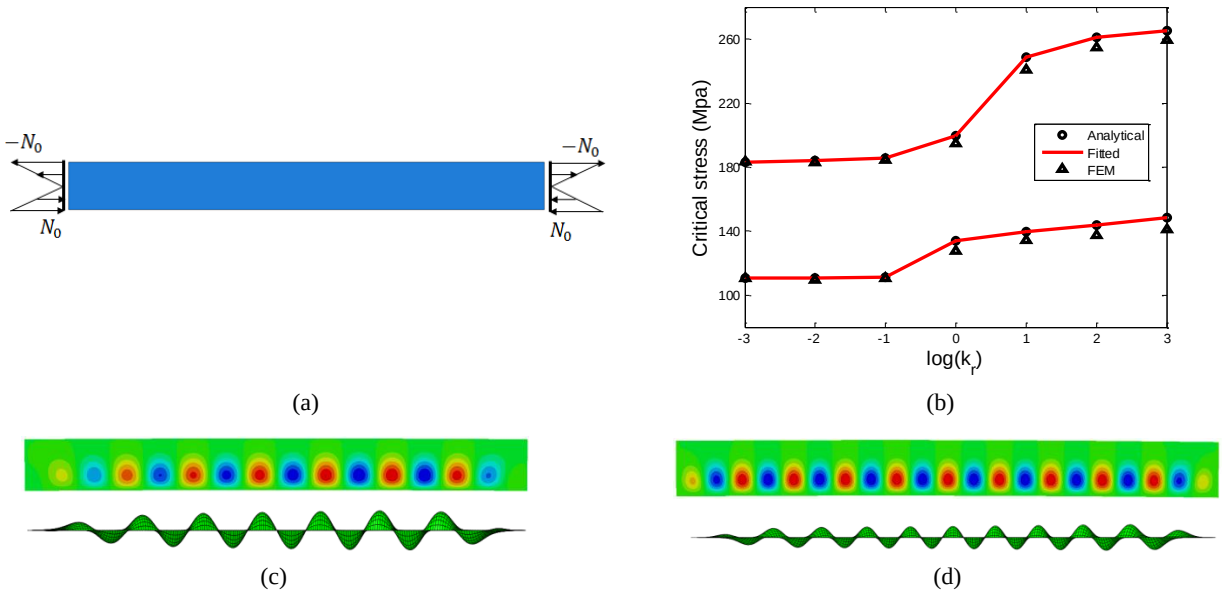

Fig. 9 Buckling coefficient and buckling model of a steel plate supported by foundation when α=2 (pure bending), (a) loading mode; (b) buckling coefficients; (c) simply supported edges and k_r = 0.001; (d) clamped edges and k_r = 0.001; (e) simply supported edges and k_r = 1; (f) clamped edges and k_r = 1; (g) simply supported edges and k_r = 1000; and (h) clamped edges and k_r = 1000

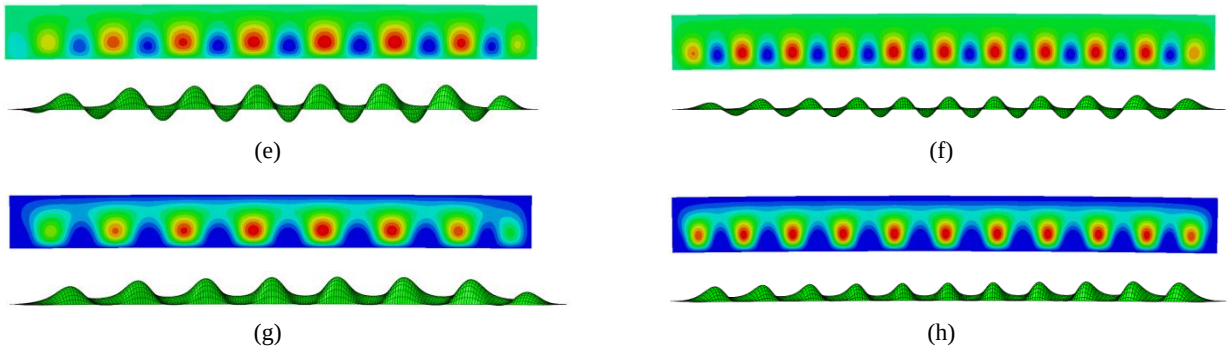

(e) (f) (g) (h)

Fig. 9 Continued

the case $\alpha = 0$. But actually, the centre line of the buckling mode shape deviates from the mid-axis $y = b/2$ slightly. The difference of centre line between $\alpha = 0$ and $\alpha = 1$ is very small. Thus, it may be deduced that the offset distance between the centre line of the buckling mode shapes and the mid-axis $y = b/2$ increases with the increase of α ($0 < \alpha < 2$). Figs. 8, 9 and 10 show that the number of half waves increases with the increasing of α value. In addition, the increasing of α value leads to a rise in the critical buckling stress (coefficient) (Table 3 and Fig. 6).

4.3.2 Effect of lateral buckling mode function g(y)

The selection of lateral buckling mode function affects the accuracy of the results. For $\alpha = 0$ (i.e., the pure uniform axial compression), only one-term approximation may be sufficient to get the accurate solution, like the one-term trigonometric function approximation for simply supported plate (Shahwan and Waas 1991, 1998) and one-term polynomial function approximation for clamped plate (Ma *et al*. 2008a). If using the hyperbolic and trigonometric function for clamped plate under pure uniform axial compression, more than one-term approximation has to be used to obtain the more accurate solution, probably three-term approximation (Fig. 3). However, for $\alpha = 2$ (i.e., the pure in-plane bending), the solution cannot be obtained if using only one term approximation (see Section 2), a higher term approximation has to be taken into account (Nölke 1937, Timoshenko and Gere 1961). At least three-term approximation has to be applied to obtain the satisfactory solution, for example, three-term trigonometric function approximation for simply supported plate and five-term hyperbolic and trigonometric function approximation for clamped plate (Fig. 3(h)). In addition, from Fig. 3(h), it can be found that the value of lateral buckling mode function $g(y)$ is zero at ~0.88 y/b. For $0 < \alpha < 2$, the term number in approximation functions should be between the two cases of $\alpha = 0$ and $\alpha = 2$ as well. In this study, two-term trigonometric function approximation is selected for simply supported plate and three-term hyperbolic and trigonometric function approximation is selected for clamped plate.

4.3.3 Effect of foundation factor k_r

Table 3 and Fig. 7 display the ratio of buckling coefficient (between $k_r \geq 1000$ and $k_r \leq 0.001$) for simply supported isotropic plate at $\alpha = 0$, $\alpha = 1$ and $\alpha = 2$ is 1.333, 1.337, and 1.374, respectively, and for clamped isotropic plate at $\alpha = 0$, $\alpha = 1$ and $\alpha = 2$ is 1.437, 1.438, and 1.450, respectively. That means by comparison with an unrestrained plate ($k_r \leq 0.001$), the critical buckling coefficient of simply supported isotropic plate with rigid foundation ($k_r \geq 1000$) increases ~33.333%, 33.664% and 37.413% at $\alpha = 0$, $\alpha = 1$ and $\alpha = 2$, respectively and clamped isotropic plate with rigid foundation ($k_r \geq 1000$) increases ~43.670 %, 43.810% and 44.981% at $\alpha = 0$, $\alpha = 1$ and $\alpha = 2$, respectively. Figs. 6 and 9 illustrate that an increase of k_r value results in the increase of the critical buckling stress. When $r = 0$, the ratio of buckling coefficient (between $k_r \geq 1000$ and $k_r \leq 0.001$) increases with the increasing of ratio of D_x/D_y and decreases with the increasing of loading parameter α (Fig. 4). Figs. 6, 8, 9 and 10 demonstrate that the size of the downward half wave decreases with the increase of foundation factor k_r, while the size of upward half waves does not reduce. This is because the elastic foundation is tensionless (see Fig. 1), if the plate goes upward and beyond the midline, the foundation has no effects and restrictions on the plate. On the contrary, if the plate goes downward and beyond the midline, the foundation has an effect on the plate, and the restriction on the plate depends on the foundation factor k_r. If $k_r = 0.001$ or < 0.001, the effect of the foundation on the plate is close to zero, so the size of upward half waves is almost equal to that of downward half waves. If $k_r = 1000$ or > 1000, the effect of the foundation is close to a rigid foundation, so downward half waves almost disappeared and only upward half waves are left. It may be concluded that the foundation stiffness has a great influence on the buckling coefficient of plate.

4.3.4 Effect of arc length along the corrugated cross section

The arc length along the corrugated cross section is a crucial factor for the corrugated plate. Arc length may affect the flexural rigidity of a corrugated plate. As presented in Eq. (46) and Table 3, it can be found that the critical buckling coefficient rises with the increase of the ratio of D_x/D_y, for the specific foundation parameter and boundary conditions.

4.3.5 Effect of boundary condition

From Table 3, when $k_r = 0$, it can be found that the ratios of buckling coefficients of an isotropic plate (between the values of clamped plates and simply supported plates) at α

= 0 and α = 1 are 1.723 and 1.737, respectively. While k_r = 1000, the ratios of buckling coefficients (clamped/simply supported) at α = 0 and α = 1 are 1.877, and 1.879, respectively. So the ratio at α = 0 is approximately equal to that at α = 1, which is in accordance with the study of Bulson (1970). When r = 0, the ratios of buckling coefficients (between the values of clamped and simply supported) are almost equal, but basically, the ratios increase with the increasing of ratio of D_x/D_y and decrease with the increasing of loading parameter α (Fig. 5). As shown in Figs. 6, 8, 9 and 10, it can be seen that the number of half waves for α = 0 is approximately equal to that for α = 1, and the number of half waves for α = 2 is more than that for α = 0 and α = 1. It can be seen that the number of half waves for simply supported plate is less than that for clamped plate. In other words, the length of half wave for plate with simply supported edges is longer than that for plate with clamped edges.

5. Conclusions

In this study, the local buckling response of an infinitely long thin corrugated plate supported by an elastic tensionless foundation under linearly varying in-plane loads was investigated. The approximate lateral buckling mode function was constructed based on the loading and boundary conditions using the energy method. The analytical solution of the critical buckling coefficient was solved for different loading factors α and boundary conditions. The approximate fitted formula of the critical buckling coefficient was developed based on the analytical solutions. A FE model of a long thin steel plate with the plate aspect ratio of 10 was developed and applied to further verify the proposed method. A series of parametric studies were implemented to investigate the influence of loading factor α, lateral buckling mode function $g(y)$, foundation factor k_r and boundary condition on the critical buckling coefficient/load. A good agreement was obtained via the comparisons of the results between the proposed method and the existing studies/FE method.

References

Altunsaray, E. and Bayer, I. (2014), "Buckling of symmetrically laminated quasi-isotropic thin rectangular plates", *Steel Compos. Struct., Int. J.*, **17**(3), 305-320

Baseri, V., Jafari, G.S. and Kolahchi, R. (2016), "Analytical solution for buckling of embedded laminated plates based on higher order shear deformation plate theory", *Steel Compos. Struct., Int. J.*, **21**(4), 883-919.

Becheri, T., Amara, K., Bouazza, M. and Benseddiq, N. (2016), "Buckling of symmetrically laminated plates using nth-order shear deformation theory with curvature effects", *Steel Compos. Struct., Int. J.*, **21**(6), 1347-1368.

Blevins, R.D. (2015), *Formulas for Dynamics, Acoustics and Vibration*, John Wiley & Sons.

Bradford, M.A., Smith, S.T. and Oehlers, D.J. (2000), "Semi-compact steel plates with unilateral restraint subjected to bending, compression and shear", *J. Constr. Steel Res.*, **56**(1), 47-67.

Bulson, P.S. (1970), *The Stability of Flat Plates*, Chatto and Windus, London, UK.

Dong, J., Zhuge, Y., Mills, J.E. and Ma, X. (2016a), "Local buckling of profiled skin sheets resting on tensionless elastic foundations under in-plane shear loading", *Eur. J. Mech. A: Solids*, **58**, 131-139.

Dong, J., Zhuge, Y., Mills, J.E. and Ma, X. (2016b), "Local buckling of profiled skin sheets resting on tensionless elastic foundations under uniaxial compression", *Thin-Wall. Struct.*, **103**, 81-89.

Dong, J., Ma, X., Zhuge, Y. and Mills, J.E. (2017), "Shear buckling analysis of laminated plates on tensionless elastic foundations", *Steel Compos. Struct., Int. J.*, **24**(6), 697-709

Dong, J., Ma, X., Zhuge, Y. and Mills, J.E. (2018a), "Unilateral contact buckling behaviour of orthotropic plates subjected to combined in-plane shear and bending", *Int. J. Solids Struct.* DOI: https://doi.org/10.1016/j.ijsolstr.2018.06.011

Dong, J., Ma, X., Zhuge, Y. and Mills, J.E. (2018b), "Local buckling of thin plate on tensionless elastic foundations under interactive uniaxial compression and shear", *Theor. Appl. Mech. Lett.*, **8**(2), 75-82.

Dong, J., Ma, X., Zhuge, Y. and Mills, J.E. (2018c), "Buckling analysis of laminated composite plate on tensionless elastic foundations under uniaxial compression", *Int. J. Struct. Stablil. Dyn.*, **18**(6), Article No. 1850079, pp. 1-21.

Harris, C.M. and Piersol, A.G. (2002), *Harris' Shock and Vibration Handbook*, Volume 5, McGraw-Hill, New York, NY, USA.

Kang, J.-H. and Leissa, A.W. (2005), "Exact solutions for the buckling of rectangular plates having linearly varying in-plane loading on two opposite simply supported edges", *Int. J. Solids Struct.*, **42**(14), 4220-4238.

Leissa, A.W. and Kang, J.-H. (2002), "Exact solutions for vibration and buckling of an SS-C-SS-C rectangular plate loaded by linearly varying in-plane stresses", *Int. J. Mech. Sci.*, **44**(9), 1925-1945.

Li, D., Smith, S. and Ma, X. (2016), "End condition effect on initial buckling performance of thin plates resting on tensionless elastic or rigid foundations", *Int. J. Mech. Sci.*, **105**, 83-89.

Liang, Q.Q., Uy, B., Wright, H.D. and Bradford, M.A. (2003), "Local and post-local buckling of double skin composite panels", *Proceedings of the Institution of Civil Engineers-Structures and Buildings*, **156**(2), 111-119.

Liang, Q.Q., Uy, B., Wright, H.D. and Bradford, M.A. (2004), "Local buckling of steel plates in double skin composite panels under biaxial compression and shear", *J. Struct. Eng.-ASCE*, **130**(3), 443-451.

Liu, Q., Qiao, P. and Guo, X. (2014), "Buckling analysis of restrained orthotropic plates under combined in-plane shear and axial loads and its application to web local buckling", *Compos. Struct.*, **111**, 540-552.

Ma, X., Butterworth, J.W. and Clifton, G.C. (2008a), "Practical analysis procedure for compressive local buckling of skin sheets in composite panels", *Int. J. Adv. Steel Constr.*, **4**(3), 230-242.

Ma, X., Butterworth, J.W. and Clifton, G.C. (2008b), "Unilateral contact buckling of lightly profiled skin sheets under compressive or shearing loads", *Int. J. Solids Struct.*, **45**(3-4), 840-849.

Nölke, K. (1937), "Biegungsbeulung der Rechteckplatte", *Arch. Appl. Mech.*, **8**(6), 403-425.

Schuette, E.H. and McCulloch, J.C. (1947), "Charts for the minimum-weight design of multiweb wings in bending", DTIC Document.

Seide, P. (1958), "Compressive buckling of a long simply supported plate on an elastic foundation", *J. Aerosp. Sci.*, **25**(6), 382-384.

Shahwan, K.W. and Waas, A.M. (1991), "Elastic buckling of

infinitely long specially orthotropic plates on tensionless foundations", *J. Eng. Mater. Technol.*, **113**(4), 396-403.
Shahwan, K.W. and Waas, A.M. (1994), "A mechanical model for the buckling of unilaterally constrained rectangular plates", *Int. J. Solids Struct.*, **31**(1), 75-87.
Shahwan, K.W. and Waas, A.M. (1998), "Buckling of unilaterally constrained infinite plates", *J. Eng. Mech.*, **124**(2), 127-136.
Smith, S.T., Bradford, M.A. and Oehlers, D.J. (1999a), "Elastic buckling of unilaterally constrained rectangular plates in pure shear", *Eng. Struct.*, **21**(5), 443-453.
Smith, S.T., Bradford, M.A. and Oehlers, D.J. (1999b), "Local buckling of side-plated reinforced-concrete beams. I, Theoretical study", *J. Struct. Eng.*, **125**(6), 622-634.
Smith, S.T., Bradford, M.A. and Oehlers, D.J. (1999c), "Local buckling of side-plated reinforced-concrete beams II, Experimental study", *J. Struct. Eng.*, **125**(6), 635-643.
Smith, S.T., Bradford, M.A. and Oehlers, D.J. (1999d), "Numerical convergence of simple and orthogonal polynomials for the unilateral plate buckling problem using the Rayleigh-Ritz method", *Int. J. Numer. Methods Eng.*, **44**(11), 1685-1707.
Smith, S.T., Bradford, M. and Oehlers, D. (2000), "Unilateral buckling of elastically restrained rectangular mild steel plates", *Comput. Mech.*, **26**(4), 317-324.
Tarján, G., Sapkás, Á. and Kollár, L.P. (2009), "Stability analysis of long composite plates with restrained edges subjected to shear and linearly varying loads", *J. Reinf. Plast. Compos.*, **29**(9), 1386-1398.
Timoshenko, S.P. and Gere, J.M. (1961), *Theory of Elastic Stability*, McGraw Hill, New York, NY, USA.
Timoshenko, S.P. and Woinowsky-Krieger, S. (1959), *Theory of Plates and Shells*, McGraw Hill, New York, NY, USA.
Wang, X., Gan, L. and Wang, Y. (2006), "A differential quadrature analysis of vibration and buckling of an SS-C-SS-C rectangular plate loaded by linearly varying in-plane stresses", *J. Sound Vib.*, **298**(1-2), 420-431.
Weaver, P.M. and Nemeth, M.P. (2007), "Bounds on flexural properties and buckling response for symmetrically laminated composite plates", *J. Eng. Mech.*, **133**(11), 1178-1191.
Wright, H. (1995), "Local stability of filled and encased steel sections", *J. Struct. Eng.*, **121**(10), 1382-1388.
Xia, Y., Friswell, M. and Flores, E.S. (2012), "Equivalent models of corrugated panels", *Int. J. Solids Struct.*, **49**(13), 1453-1462.
Ye, Z., Berdichevsky, V.L. and Yu, W. (2014), "An equivalent classical plate model of corrugated structures", *Int. J. Solids Struct.*, **51**(11), 2073-2083.

BU